Multi-Wavelength Single-Shot Interferometry

Katsuichi Kitagawa
R&D Center, Electronics Division
Toray Engineering Co., Ltd.
Otsu, Japan
katsuichi_kitagawa@toray-eng.co.jp

***Abstract*— A new surface profiling technique is proposed, which enables us fast and robust 3D measurements with interferometric resolution and extended measurement range. It is accomplished by a newly developed multi-wavelength imaging system, which is easily and economically constructed by a commercially available RGB LED illuminator and a color camera. With this imaging system, we first developed a two-wavelength single-shot technique. Then we expanded it to three wavelengths and successfully measured a step height of 1000nm. For this purpose, we developed several algorithms including crosstalk compensation and frequency estimation. The algorithms and experimental results are presented.**

Keywords-interferometry; single-shot; surface profiler; multi-wavelength; three-wavelength.

I. INTRODUCTION

The measurement accuracy of interferometric surface profiling is generally limited by the environmental vibration. This is because the conventional methods need multiple images with different reference positions.

To overcome this problem, single-shot interferometry, which can measure the surface profile from a single image, has been proposed. A typical example is spatial carrier interferometry, in which carrier fringes are introduced by tilting the reference mirror (Fig. 1). From a single interferogram, the phase distribution can be calculated by the Fourier-transform method [1] or the spatial synchronous method [2-3]. However, the Fourier-transform method has the disadvantages of complexity and a long computation time, and both methods use integral transforms, which filter out the high-frequency components, resulting in corner-rounding effects and low spatial resolution.

To solve these problems, we have proposed a new algorithm called Local Model Fitting (LMF) method [4]. It will be used in this work to extract the phase distribution from two-dimensional fringe patterns.

However, all methods using a single wavelength have the same limitation: the maximum difference of the surface height between two adjacent pixels must be less than $\lambda/4$, where λ is the wavelength of the light source.

A common approach to alleviating this problem is to use multi-wavelength interferometry. This technique has been popular in phase-shifting interferometry [5]. However, its combination with single-shot interferometry is not so easy, because its imaging system must capture multiple interference fringe patterns with different wavelengths simultaneously.

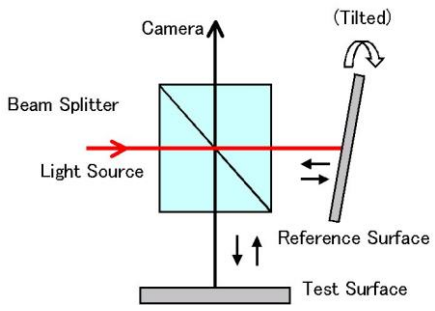

Figure 1. Optics of spatial carrier method.

Onodera and Ishii [6] proposed two-wavelength interferometry based on the Fourier-transform method. Two lasers, YAG and He-Ne, were used to illuminate an interferometer simultaneously, and a single fringe image was captured. However, since the imaging device was a monochromatic CCD camera, only the synthetic phase was obtained under the assumption that two modulation intensities were equal; i.e., the two individual phases were not obtained.

Schmidt [7] combined two-wavelength interferometry with spatial carrier phase-shifting interferometry. Two images were acquired by changing an optical filter. This means that this method is not a single-shot method. Another problem is its requirement of setting the correct carrier frequency of the fringes for both wavelengths.

This paper proposes a new imaging system for multi-wavelength single-shot interferometry, which allows us to simultaneously capture three images at different wavelengths. With this imaging system, we first developed a two-wavelength single-shot technique and successfully measured a 350nm step height [8]. Then we expanded it to three wavelengths and measured a 1000nm step height. Thus, our new system can achieve a wider measurement range while maintaining its robustness against vibration.

II. MULTI-WAVELENGTH IMAGING SYSTEM

In order to capture multiple interference fringe patterns with different wavelengths simultaneously, we propose a three-wavelength imaging system that uses three LEDs and a color camera. A similar system for three-wavelength phase-shifting

interferometry reported by Pfortner and Schwider [9] uses three lasers (HeNe: 633 nm, NdYAG: 532 nm, NdYAG: 473 nm) with rotating scatterers that destroy the spatial coherence of the laser lights. Another example is a system by Baugh, Swenson and Talke [10]. It is for head/tape spacing measurement, and uses three white-light sources, each with a different interference filter.

Compared with these systems, our system is inexpensive and compact. It is easily constructed by a commercially available RGB LED illuminator (CCS, HLV-3M-RGB-3W) and a color camera (Basler, sca640-70gc). Fig. 2 shows the picture of the illuminator we used. Its optical specifications are shown in Table I.

TABLE I. SPECIFICATIONS OF THE ILLUMINATOR

Color	Wavelength (nm)	Bandwidth (nm)
R	627	20
G	530	35
B	470	25

Fig. 3 shows the spectral sensitivity of the color CCD camera we used, with the spectral peaks of three LEDs. From the captured color image, we extracted interference fringe patterns with different wavelengths. It is noted that when only the red and blue LEDs were used, we could obtain a 470nm image from the B-component and 627nm image from the R-component with almost no crosstalk. Therefore, we first developed a two-wavelength single-shot technique, and then expanded it to three wavelengths.

III. TWO-WAVELENGTH SINGLE-SHOT METHOD

A. Algorithm

As mentioned in the previous section, we could obtain a 470nm image from the B-frame and a 627nm image from the R-frame by turning on only the blue and red LEDs. The phase at each pixel was calculated by the Local Model Fitting (LMF) method [4]. Its summary is shown in the Appendix.

Once two phases (ϕ_1, ϕ_2) have been obtained for the two wavelengths (λ_1, λ_2), we can use two-wavelength unwrapping algorithms in the phase-shifting interferometry. The simplest one is the equivalent wavelength method [5], in which the height is calculated by using an equivalent wavelength λ_{eq} defined by $\lambda_{eq} = \lambda_1 \lambda_2/(\lambda_2 - \lambda_1)$. By this method, the height-step condition for a correct phase-unwrapping is expanded from $\lambda_1/4$ to $\lambda_{eq}/4$.

B. Experiments

In order to demonstrate the validity of the proposed method, we performed an interferometric test using a Toray Engineering SP-500 surface profiler [11], shown in Fig. 4, which incorporates a Michelson interferometric microscope. The illumination unit and the camera were replaced by our proposed ones.

Since the equivalent wavelength of 470 nm and 627 nm is 1877 nm, the height gap between adjacent data points can be as large as 469 nm without any ambiguities. Therefore, we chose

Figure 2. RGB LED Illuminator.

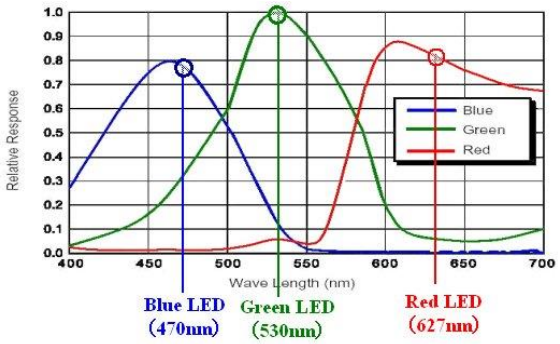

Figure 3. Spectral curves of LEDs and color camera.

Figure 4. Toray Engineering SP-500 surface profiler.

a patterned quartz plate with a nominal step height of 350 nm as the test sample.

Fig. 5 shows the captured color image. The spatial carrier frequencies were estimated for each wavelength from the horizontal fringe counts. The number of vicinity data points in the LMF calculation was 25 (horizontal) × 5 (vertical).

From the two unwrapped phase data, we obtained surface profiles using the algorithm mentioned in the previous section. Fig. 6 presents the 3D measurement results. The results agree well with those of the conventional method.

IV. THREE-WAVELENGTH SINGLE-SHOT METHOD

A. Algorithm

For a larger range of unambiguity, three-wavelength interferometry was investigated. The imaging system is

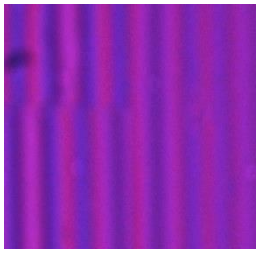

Figure 5. Captured color image by two-wavelength imaging system.

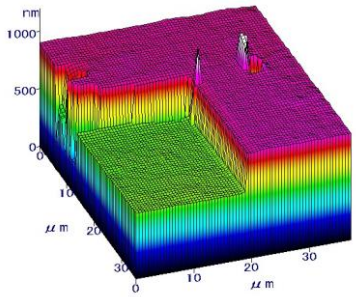

Figure 6. 3D surface profiles by two-wavelength single-shot method.

described in section 2. Many issues must be resolved for three-wavelength interferometry. Fig. 7 shows the flowchart for three-wavelength interferometry. We describe the algorithms step by step below.

1) Crosstalk compensation

When three wavelengths are used, the crosstalk between B, G, and R signals is not negligible. From Fig. 3, it is estimated that the crosstalk from the B illumination to the G signal is the largest.

To compensate for the crosstalk, we assumed the following linear model:

$$\begin{cases} B' = B + aG + bR \\ G' = cB + G + dR \\ R' = eB + fG + R, \end{cases} \tag{1}$$

where *B'*, *G'*, and *R'* are the observed values, *B*, *G*, and *R* are the true values, and *a*, *b*, *c*, *d*, *e*, and *f* are the crosstalk coefficients.

Since the coefficients are small enough, we can ignore their product terms. Then the true values are given by

$$\begin{cases} B = B' - aG' - bR' \\ G = -cB' + G' - dR' \\ R = -eB' - fG' + R'. \end{cases} \tag{2}$$

The method to obtain the coefficients is shown in section *B.2)*.

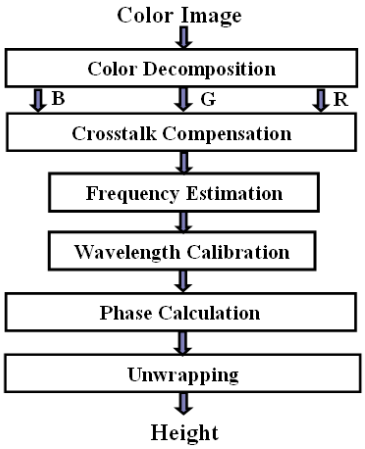

Figure 7. Flowchart of three-wavelength interferometry.

2) Frequency estimation

For the three-wavelength unwrapping described below, an accurate estimation of the fringe frequency is essential, because any error causes an error in phase calculation and then in fringe order estimation.

The most common method used in frequency estimation seems to be the Fourier transform. However, its computational cost would be very high if high accuracy were required.

To solve this problem, we devised a new carrier fringe frequency estimation method, named the phase gradient method, which is based on the relation between the frequency error and the phase. Although this technique is applicable to 2-dimensional estimation, its principle is described at first for 1-dimensional estimation.

Let the observed sinusoidal signal $g(x)$ be expressed by

$$g(x) = A\cos(2\pi fx + \phi(x)), \tag{3}$$

where f is the frequency to be estimated.

To the observed data, we fit the following model function using the least squares method:

$$g'(x) = A'\cos(2\pi f_0 x + \phi'(x)), \tag{4}$$

where f_0 is an initial guess at the frequency.

For this procedure, the LMF method can be applied, and phase $\phi'(x)$ is experimentally obtained.

On the other hand, from (3) and (4), we obtain

$$\phi'(x) = 2\pi(f - f_0)x + \phi(x). \tag{5}$$

This means that in a flat area, where $\phi(x)$ =constant, $\phi'(x)$ is proportional to x as shown in Fig. 8, and the phase

gradient $d\phi'/dx$ is dependent on the frequency error (f - f_0). Therefore, the frequency can be estimated by

$$f = f_0 + (d\phi'/dx)/2\pi. \quad (6)$$

Next, we expanded this algorithm to two dimensions. In two dimensions, (5) becomes

$$\phi'(x,y) = 2\pi(f_x - f_{x0})x + 2\pi(f_y - f_{y_0})y + \phi(x,y). \quad (7)$$

Then the equation for frequency estimation is obtained as

$$\begin{cases} f_x = f_{x0} + (d\phi'(x,y)/dx)/2\pi \\ f_y = f_{y_0} + (d\phi'(x,y)/dy)/2\pi. \end{cases} \quad (8)$$

Computer experiments have proved that this method is very accurate, robust and fast.

3) Wavelength calibration

Using the obtained fringe frequency data, we could calibrate the three wavelengths because the fringe frequency f is inversely proportional to the wavelength λ. One wavelength is selected as a standard wavelength λ_0; then the other two wavelengths λ_i are calculated from their frequencies f_i by

$$\lambda_i = (f_0/f_i)\lambda_0, \quad (9)$$

where f_0 is the frequency of the standard wavelength.

This wavelength calibration is essential because the precise center wavelengths of the LEDs are unknown and their error can cause an error in three-wavelength unwrapping.

4) Phase calculation

The phase at each pixel is calculated by the LMF method [4], summarized in the Appendix.

5) Three-wavelength unwrapping

For three-wavelength unwrapping, several algorithms have been proposed. Among them, the exact fraction method [9,12] is simple and easy to understand. Its principle is shown in Fig. 9. The height can be expressed as

$$h_i(n_i) = (\phi_i/2\pi + n_i)\cdot(\lambda_i/2), \quad (10)$$

where i is the wavelength (i=1,2,3), ϕ_i is the phase, n_i is the interference order, and λ_i is the wavelength.

The unknown interference orders n_i are determined so that the three candidate heights (h_1, h_2, and h_3) match best. As the degree of matching, the range (= difference between the maximum and minimum values) can be used. The optimum orders n_i are searched within a limited integer range which corresponds to the expected height range.

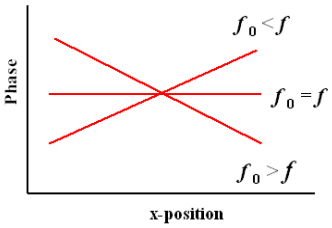

Figure 8. Relation between phase and frequency error.

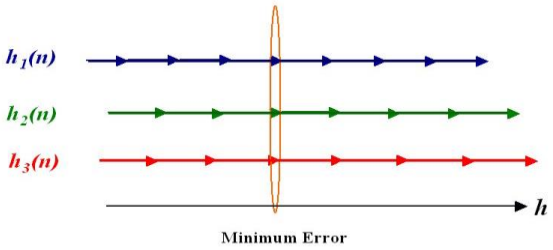

Figure 9. Principle of exact fraction method.

B. Experimental Results

We performed an interferometric test with the same setup as with two wavelengths. As the test sample, we chose a patterned quartz plate with a nominal step height of 1000 nm.

1) Image capturing

Fig. 10 shows the captured color image and Fig. 11 shows the extracted B, G and R components.

2) Crosstalk compensation

The crosstalk coefficients were obtained by the following experiment. By turning on only one LED, for example, B-LED, and capturing a color image, we made the regression analysis shown in Fig. 12. From the regression coefficients, the crosstalk coefficients between B and G and between B and R were obtained as 0.28 and 0.01, respectively. From similar experiments, the coefficient matrix was obtained as follows:

$$\begin{pmatrix} 1 & 0.05 & 0.00 \\ 0.28 & 1 & 0.04 \\ 0.01 & 0.04 & 1 \end{pmatrix}$$

Using these coefficients, crosstalk compensation was made. Fig. 13 shows the G waveforms before and after the compensation. The beat frequency observed before the compensation disappears after the compensation. This effect is also confirmed by the spectral analysis shown in Fig. 14, which was obtained by FFT operation of the waveform signals. The B component peak near 480 nm is deleted by the compensation.

3) Frequency estimation

By the phase gradient method shown in section *A.2)*, the carrier fringe frequencies were estimated. The standard area was chosen within the upper flat area of 400×200 pixels. The phase was calculated by the LMF method with a data size of 25×5 pixels. Two-dimensional phase unwrapping was made by the MST (Minimum Spanning Tree) method [13]. The results are shown in Table II.

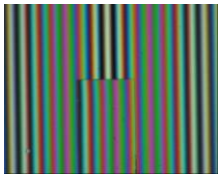

Figure 10. Captured color image.

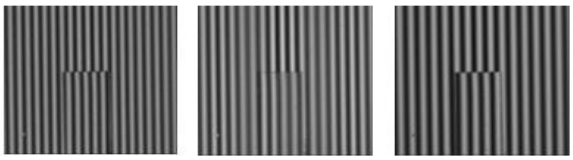

(B) (G) (R)

Figure 11. Extracted three components.

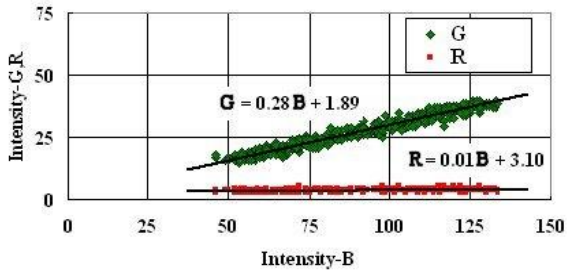

Figure 12. Regression analysis between B and G, R.

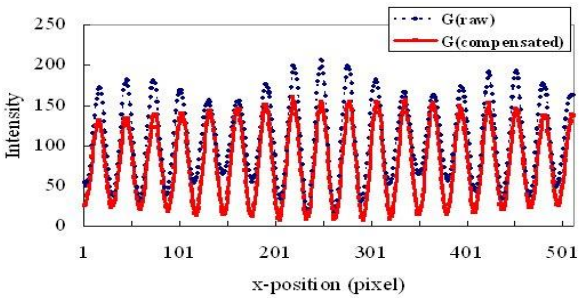

Figure 13. Effect of crosstalk compensation: Change of waveform.

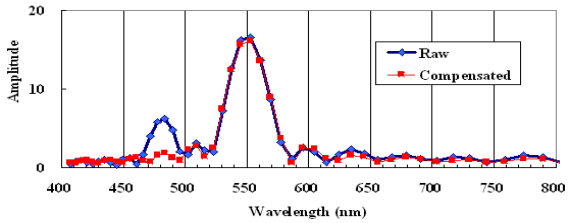

Figure 14. Effect of crosstalk compensation: Change of spectrum.

TABLE II. ESTIMATED FREQUENCIES

Color	f_x (1/pix)	f_y (1/pix)
B	0.0394	0.0005
G	0.0343	0.0005
R	0.0301	0.0004

4) Wavelength calibration

Using the obtained fringe frequency data, we calibrated two wavelengths of B and G relative to R. The result is shown in Table III.

TABLE III. RESULT OF WAVELENGTH CALIBRATION

Color	Calibrated Wavelength (nm)	Nominal wavelength (nm)
B	478.5	470
G	548.9	530
R	(627)	627

5) Phase calculation

The phase at each pixel is calculated by the LMF method. The data size is 25×5 pixels. The obtained phase profiles at the y=360 line are shown in Fig. 15. Please note that there appears no tilt because of the correct frequency estimation.

6) Height calculation

From the phase data, the height at each point was calculated by the exact fraction method. The height profile along the y=360 line is shown in Fig. 16. The three dimensional height is shown in Fig. 17. The 1000 nm step height was measured

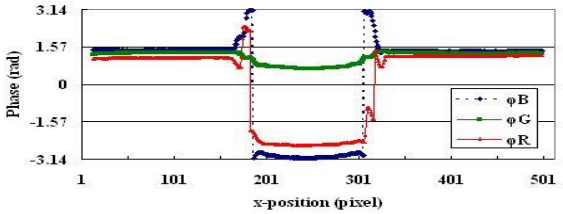

Figure 15. Phase profiles at y=360.

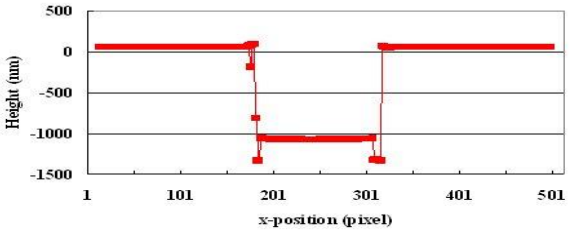

Figure 16. Height profile at y=360.

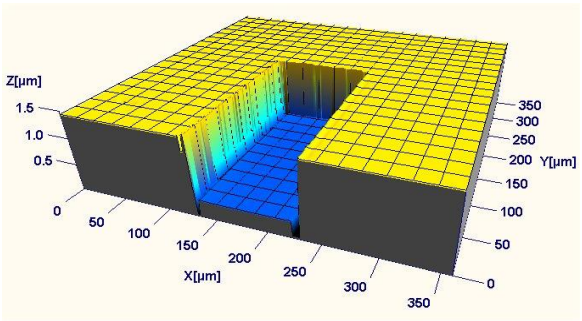

Figure 17. 3D view of measurement result.

correctly. The total calculation time for 512×480 pixels was 1.18 sec with a laptop PC (Pentium 1.6GHz). The repeatability (sigma) was on the order of a few nm.

V. CONCLUSION

We have proposed a new surface profiling technique, the Multi-Wavelength Single-Shot method, which enables us to measure a surface profile with an extended phase measurement range. It is accomplished by a newly developed multi-wavelength imaging system, which is easily and economically constructed from a commercially available RGB LED illuminator and a color camera.

For two-wavelength interferometry, only B and R LEDs are used. In this case, the crosstalk is negligible. The phases are calculated by using the LMF algorithm. Then the height is obtained by the equivalent wavelength method. A 350 nm step height was successfully measured without phase ambiguity.

For three-wavelength interferometry, all B, G and R LEDs are used. In this case, the crosstalk is not negligible, so a crosstalk compensation algorithm was devised. Before the phase calculation, the fringe frequencies had to be accurately determined, because even a small error in frequency estimation can result in the faulty determination of final fringe orders. For this purpose, a new frequency estimation algorithm was devised. From the obtained three phases, the height was calculated by the exact fraction method. A 1000 nm step height was successfully measured without phase ambiguity.

The experimental results demonstrated that the proposed method can measure a surface profile fast and accurately from a single color image, with an extended measurement range.

APPENDIX
LOCAL MODEL FITTING ALGORITHM

In this section, we give a short review of the local model fitting (LMF) algorithm proposed in [4].

When we tilt the reference mirror, the observed signal is given by

$$g(x,y) = a(x,y) + b(x,y)\cos\left(\phi(x,y) + 2\pi f_x x + 2\pi f_y y\right), \quad \text{(A.1)}$$

where $a(x,y)$ and $b(x,y)$ are the bias and the amplitude. The function $\phi(x,y)$ contains the information on the surface profile that we would like to extract. Variables f_x and f_y stand for the spatial carrier frequencies along the x- and y-axes, respectively.

Here we make the following assumption: $a(x,y)$, $b(x,y)$, and $\phi(x,y)$ are constant in the vicinity of (x_0, y_0); i.e., our local model is

$$g(x,y) = a + b\cos(\phi + 2\pi f_x x + 2\pi f_y y), \quad \text{(A.2)}$$

or equivalently

$$g(x_i,y_i) = a + \xi_c\phi_c(x_i,y_i) + \xi_s\phi_s(x_i,y_i), \quad \text{(A.3)}$$

where $\xi_c = b\cos\phi$, $\xi_s = b\sin\phi$, $\phi_c(x,y) = \cos\left(2\pi f_x x + 2\pi f_y y\right)$ and $\phi_s(x,y) = -\sin\left(2\pi f_x x + 2\pi f_y y\right)$.

Then the unknowns in (A.3) can be determined by solving the following least squares problem:

$$(a,\xi_c,\xi_s) = \underset{(a,\xi_c,\xi_s)}{\operatorname{argmin}} \sum_{i=1}^{n} \left[g(x_i,y_i) - a - \xi_c\varphi_c(x_i,y_i) - \xi_s\varphi_s(x_i,y_i)\right]^2. \quad \text{(A.4)}$$

Since the above model is linear, we can easily obtain the closed-form solutions $\hat{a}$, $\hat{\xi}_c$, and $\hat{\xi}_s$. Then we can obtain an estimate ϕ by

$$\hat{\phi} = \arctan\left(\hat{\xi}_s / \hat{\xi}_c\right) \quad \text{(A.5)}$$

REFERENCES

[1] M. Takeda, H. Ina, and S. Kobayashi, "Fourier-transform method of fringe-pattern analysis for computer-based topography and interferometry", J. Opt. Soc. Am., Vol. 72, No. 1, pp. 156-160, 1982.

[2] S. Toyooka and M. Tominaga, "Spatial fringe scanning for optical phase measurement", Opt. Commun. , Vol. 51, No. 2, pp. 68-70, 1984.

[3] K. H. Womack, "Interferometric phase measurement using spatial synchronous detection", Opt. Eng. Vol. 23, pp. 391-395, 1984.

[4] M. Sugiyama, H. Ogawa, K. Kitagawa, and K. Suzuki, "Single-shot surface profiling by local model fitting", Appl. Opt., Vol. 45, No. 31, pp. 7999-8005, 2006.

[5] Y.Y. Cheng and J.C. Wyant, "Two-wavelength phase-shifting interferometry", Appl. Opt., Vol. 23, pp. 4539-4543, 1984.

[6] R. Onodera and Y. Ishii, "Two-Wavelength Interferometry That Uses a Fourier-Transform Method," Appl. Opt. Vol. 37, pp. 7988-7994, 1998.

[7] J. Schmidt: "Two-wavelength interferometry combined with N-point technique", Proc. SPIE, 3744, pp. 200-206, 1999.

[8] K. Kitagawa, M. Sugiyama, T. Matsuzaka, H. Ogawa, and K. Suzuki: "Two-Wavelength Single-Shot Interferometry", Proc. of SICE Annual Conference 2007, pp.724-728.

[9] A. Pfortner and J. Schwider: "Red-green-blue interferometer for the metrology of discontinuous structures", Appl. Opt., Vol. 42, pp. 667-673, 2003.

[10] E. Baugh, J. Swenson and F.E. Talke, "Simultaneous three-wavelength interferometry for head/tape spacing measurement", J. Tribol., Vol. 120, pp. 549-553, 1998.

[11] Toray Inspection Equipment Home Page, (Toray Engineering Co., 2009), http://www.scn.tv/user/torayins/

[12] K. Iwata, J. Zhang, and H. Kikuta: "Consideration of fractional fringe method on the basis of the least squares method", Optical Review, Vol. 10, pp. 202-205, 2003.

[13] M.Takeda and T.Abe: "Phase unwrapping by a maximum cross-amplitude spanning tree algorithm: a comparative study", Opt. Eng., Vol. 35, pp. 2345-2351, 1996.

This is the final manuscript of
Katsuichi Kitagawa: "Multi-Wavelength Single-Shot Interferometry", ISOT 2009 (International Symposium on Optomechatronic Technologies) (Sept. 2009; Istanbul)
http://ieeexplore.ieee.org/xpl/freeabs_all.jsp?arnumber=5326095